ELSEVIER

Physica D 133 (1999) 1–17

PHYSICA D

www.elsevier.com/locate/physd

Predictability and granular materials

R.P. Behringer [a,*], Daniel Howell [a], Lou Kondic [a], Sarath Tennakoon [a], Christian Veje [b]

[a] *Department of Physics and Center for Nonlinear and Complex Systems, Duke University, Durham, NC 27708-0305, USA*

[b] *Niels Bohr Institute, Copenhagen, Denmark*

Abstract

Granular materials present a number of challenges to predictability. The classical description of a dense granular material is based on Coulomb friction. For a static array of grains, the Coulomb friction forces are typically underdetermined. If we are to make useful statements about such arrays, we must develop new approaches, including the development of statistical descriptions. Granular materials also show large fluctuations in the local forces. These fluctuations are quite sensitive to small perturbations in the packing geometry of the grains. In the past, they have typically been ignored. However, recent experiments and models are beginning to shed new light on their characteristics. This article briefly reviews some of this new work, and in particular presents experimental results characterizing fluctuations and the role of friction in granular materials.

Keywords: Granular materials; Stress chains; Fluctuations; Friction

1. Introduction

Granular materials surround us everywhere in daily life, and present a variety of fascinating dynamic and static phenomena [1–7]. Common examples of these materials include sand, soils, coal, grains, cereal, ores, pharmaceutical powders, pills, even dog food. Granular materials can behave like solids – a heap is stable up to some angle of repose – but they can also flow, at least heuristically, like fluids. For instance, once a heap is raised past the maximum stability angle, avalanches occur. And, shaken granular materials can convect, exhibit traveling waves, and standing wave patterns that bear a remarkable resemblance to patterns seen in Rayleigh–Bénard convection.

However, our ability to predict the state of a granular material lags far behind our ability to predict the dynamics of ordinary fluids. There are a number of reasons for this, including unpredictability associated with static friction and strong fluctuational effects. Here, we will try to give some insight into the difficulties, and we will discuss recent work that is providing new insights that may resolve some of these difficulties.

At the most fundamental level, the interaction forces between grains are relatively simple ones. These include hard body interactions (to a first approximation), friction, and inelasticity, as characterized by a coefficient of restitution,

* Corresponding author.

0167-2789/99/$ – see front matter
PII: S0167-2789(99)00094-9

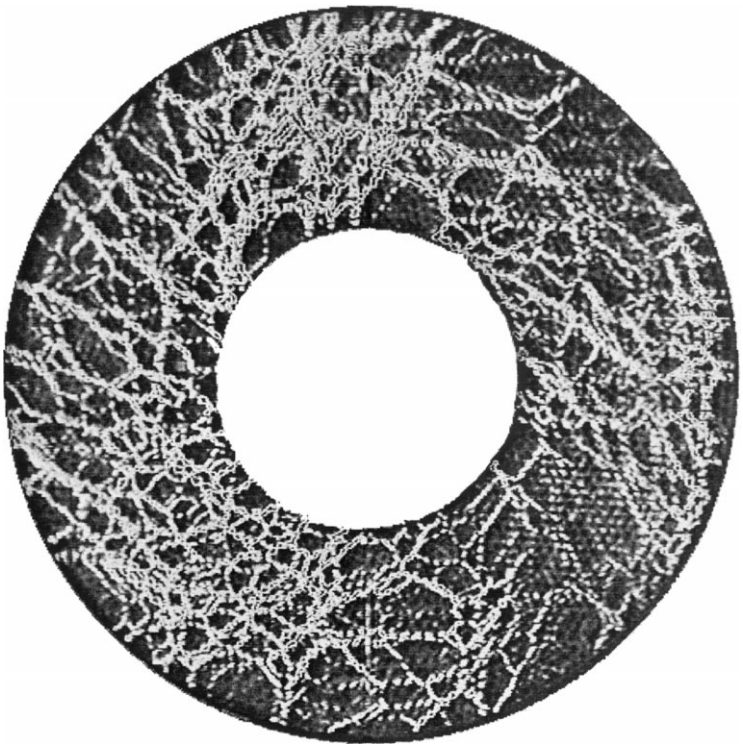

Fig. 1. Image showing stress chains for a large packing fraction, $\gamma \simeq 0.80$.

$e < 1$. One might imagine that a granular material resembles a hard sphere gas, with the additional complication of dissipation.

Although these forces seem simple, they lead to indeterminancy and to complex dynamics that cannot be treated in the framework of ordinary statistical mechanics [8–10]. Due to the dissipative nature of the interactions, even an initially energetic collection of grains quickly coalesces into a dense compact state, so that the concept of ordinary temperature no longer applies, although it is still possible to consider a "granular temperature" defined in terms of the fluctuation components of the kinetic energy [11]. Such a compact state is typically highly inhomogeneous with regard to the forces experienced by individual grains. These forces are carried preferentially on a complex spatial network known as stress chains. Fig. 1 shows an experimental realization of these chains for a 2D granular system that is discussed in more detail below. In this figure, the "grains" (in this case disks) that are carrying the largest force appear the brightest. It is visually clear that this system is not homogeneous as far as force is concerned. A key point is that if grains are displaced by a very small amount, the stress chains will change dramatically [12]. Thus, even moderate uncertainty in the grain configurations is sufficient to lead to large uncertainty in the force configuration. If the systems is driven, for instance by slow shearing, the stress chains evolve in a complex random way [13].

Classical Coulomb friction is an important source of intrinsic unpredictability for granular systems [14,15]. Some simple examples give insight into the origin of this indeterminancy associated with Coulomb friction. For example, suppose that a block rests on an inclined surface at an angle θ to the horizontal, with an additional unknown force applied along the incline. Coulomb friction is not able to predict the value of the unknown force, since there is a range of forces which would allow the block to remain at rest on the surface. An example that is particularly

germane to granular systems consists of asking when a frictional system on an inclined surface with slope $\tan\theta$ will just begin to slip. For one particle, a block, the answer is easy: Coulomb friction is just able to sustain the block at rest for $\tan\theta = \mu_s$, where μ_s is the coefficient of static friction. In this case, there are two unknown forces, one normal and one tangential to the contact surfaces, and two constraints if the block does not slide. (The process is more complex if we consider that the block might also rotate.) Now consider two disks in mutual contact resting on an inclined plane. We imagine that these disks were placed on the plane and that θ was gradually increased just to the point of slipping. As in the first example, the forces are determined because there are now six unknown forces and torques that are matched with the six force and torque balance conditions on the two disks. However, if we augment the system to $N = 3$ particles, there are now $3N = 9$ static balance conditions, but 10 unknown forces at the 5 contacts. Thus, there is a continuous range of forces that satisfies the static balance conditions. If more particles are added, the situation is typically worse. Each new grain implies two new contacts (in 2D) hence four unknown forces. Force and torque balance applied to this disk provides only three additional constraints.

In the past, it has often been assumed that fluctuations in static or slowly evolving systems were small on the scale of the system of interest. This may be true on very large scales such as a large soil embankment. However, it is less clear that this must be so in other commercially important systems. For instance, if large chunks of coal, with a typical size of 10 cm are in a silo with a diameter of 20 m, there are then only 200 particles across the diameter, which is not much larger than chain lengths seen in some experiments.

In particular, some older experiments [16–18] as well as several experiments in the past few years indicated that fluctuations can be significant on scales of tens to hundreds of grains. In one of these, Liu and Nagel [12] measured the propagation of sound through an array of grains. Sound was injected through a loudspeaker and detected by a microphone in the material. The frequency dependence of the detected sound was complicated but reproducible as long as the arrangement of the particles was undisturbed. However, a minute perturbation of the particle arrangement was sufficient to significantly change the frequency response.

In another set of experiments, Baxter et al. [19,20] measured the acoustic transmission at the side of a small hopper during outflow of material. Here, the goal was to test for a characteristic time scale, τ, predicted on the basis of continuum models [21]. However, the detected signal was very noisy, and a power spectrum from this signal was roughly a power law in the frequency, $P(\omega) \propto \omega^{-\alpha}$. For various conditions, the exponent α lay in the range $1.3 \leq \alpha \leq 2.3$. By contrast, the expected response would have involved a broadened peak in the vicinity of a frequency $\sim \tau^{-1}$. More recently, experiments on shearing [22], discussed here, on compression [23], and on forces in bead packs near boundaries [24] have also demonstrated strong fluctuations.

Until recently, models for slow flows in granular materials have neglected fluctuations. However, there have been several new models [25–30] that consider fluctuations. These models fall into two classes. The first is based on lattice models, where grains are placed (with the possible exception of vacancies [28]) on a regular lattice. The unknown/random nature of the contacts is introduced by "propagating" forces through the lattice so that the forces and torques on a particle are provided from neighbors in a random way, but such that some or all of the forces and torques are in balance. Roughly speaking, these models predict exponential distributions of the force on a single grain, at least for large forces, unless there are sufficiently many defects in the lattice. For instance, in the q-model of Coppersmith et al. the distribution of forces is given by $\rho_q \propto F^{N-1}\exp(-F/F_o)$, where N is the dimension of the system, and F_o is determined by the applied force. The other class of model is contact dynamics [30] in which the frictional uncertainty is resolved by allowing the system to relax dynamically. Again, this model predicts essentially exponential distributions of forces at large F. Such distributions have been observed in recent experiments [24,25].

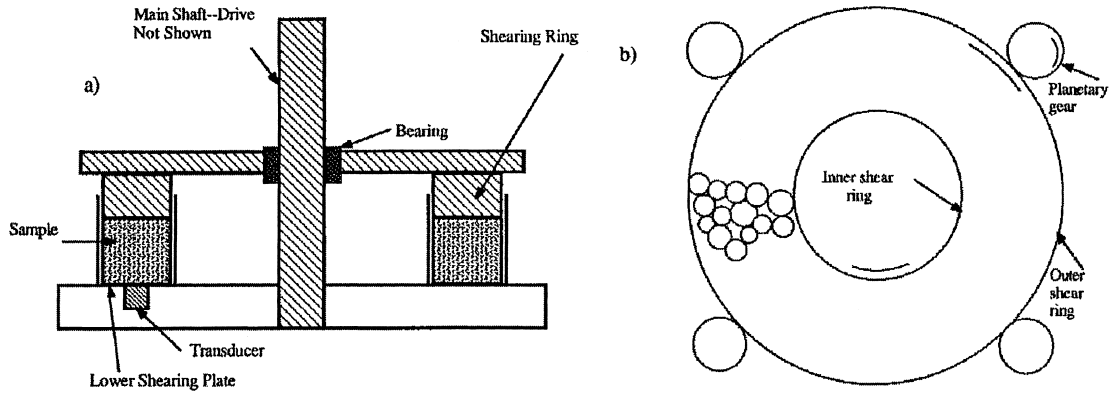

Fig. 2. Schematics of the 3D (a) and 2D (b) Couette experiments. The former is a vertical cross section of a system with cylindrical symmetry.

2. Experiments on stress fluctuations

2.1. Stress measurements in 3D

More recently, we have probed the fluctuations associated with slow shearing for both 3D and 2D Couette flows [13,22]. In the first of these experiments, we sheared glass spheres in a 3D annular channel. A sketch of the apparatus is given in Fig. 2(a) which gives a vertical cross section of the apparatus which has cylindrical symmetry in the horizontal plane. The spheres were placed in the annular channel and sheared from above by a roughened rotating ring. Stress was transmitted through this system to the base, in which a normal stress transducer was embedded. There was necessarily always slipping of grains somewhere in the layer, and the experiment was run for long times during which data was collected at a rate of 500 Hz to 1 kHz.

Data were obtained over a broad range of ring rotation frequencies, $\omega_r \equiv \dot{\theta}$, and for a range of particle sizes, $1\,\text{mm} \leq d \leq 5\,\text{mm}$. The effective cross sectional area of the detector was $0.8\,\text{cm}^2$, so that as we varied d, the number of particles contacting the detector varied from ~ 100 to ~ 4. In this way, we could probe correlational effects. For instance, in the original q-model, there are no correlations between particles.

A typical example of the resulting time series is given in Fig. 3. There are noisy fluctuations in the stress, but more importantly, these fluctuations can be much larger than the mean, which is indicated in the figure by the small bar at the lower left. This time series is for relatively large particles, $d = 4\,\text{mm}$, but the qualitative nature of the data for smaller d is similar.

It is useful to examine the power spectra of these data, and a typical set of results is given in Fig. 4. The spectra fall off at large ω as ω^{-2}, but vary roughly as $\omega^{-\alpha}$ with $\alpha < 2$ below some characteristic frequency, ω_c that depends on the shearing rate, $\dot{\theta}$. These data also have an interesting rate-independence that suggest that the system is close to static equilibrium. Specifically, if the stress time series data depended on time only as $\sigma = f(\dot{\theta}t)$, then the scaled power, $\dot{\theta}P$ as a function of scaled frequency, $\omega/\dot{\theta}$ should be independent of $\dot{\theta}$. Fig. 5 shows that this kind of rate independence applies. This figure shows scaled power vs. scaled frequency for two different size particles. An inspection of the figure shows that the scaling is quite good for a given particle size and layer height, h. Also, this figure demonstrates that the measured fluctuational stress is not a strong function of the particle size. This is surprising because we would expect that there would be significant reduction of the fluctuations due to averaging in the case of the smaller particles, because there are many more particles in contact with the detector than for the larger particles. This suggests that there are strong stress chains that provide much of the force impinging on the detector, and that the remainder of the grains carry only a modest amount of the stress.

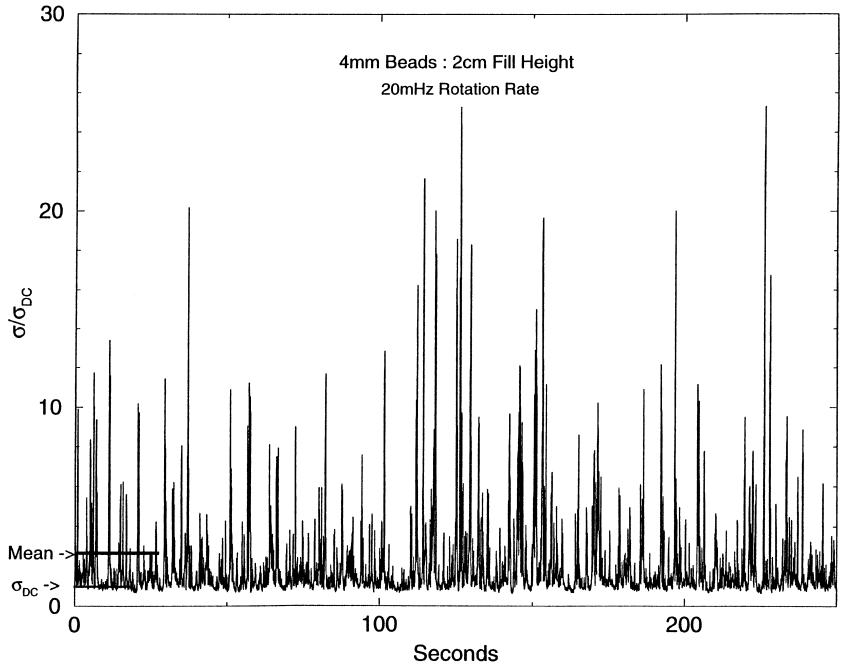

Fig. 3. Typical time series for the normal stress as a function of time, for $d = 4\,\text{mm}$ and $\dot{\theta}/(2\pi) = 20\,\text{mHz}$. The data are normalized by the DC stress which we measure in the absence of shearing. The horizontal line indicates the mean.

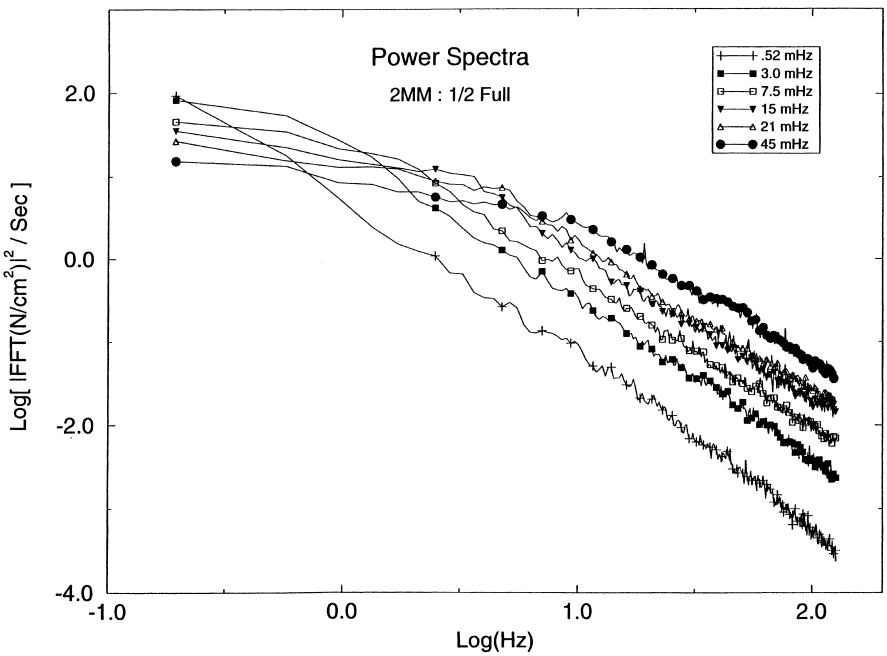

Fig. 4. Representative spectra for $d = 2\,\text{mm}$. The rotations rates, $\dot{\theta}$ (normalized by 2π) of the shearing ring are noted in the upper corner. At high ω, the spectra vary as ω^{-2}, and more weakly with ω at low ω.

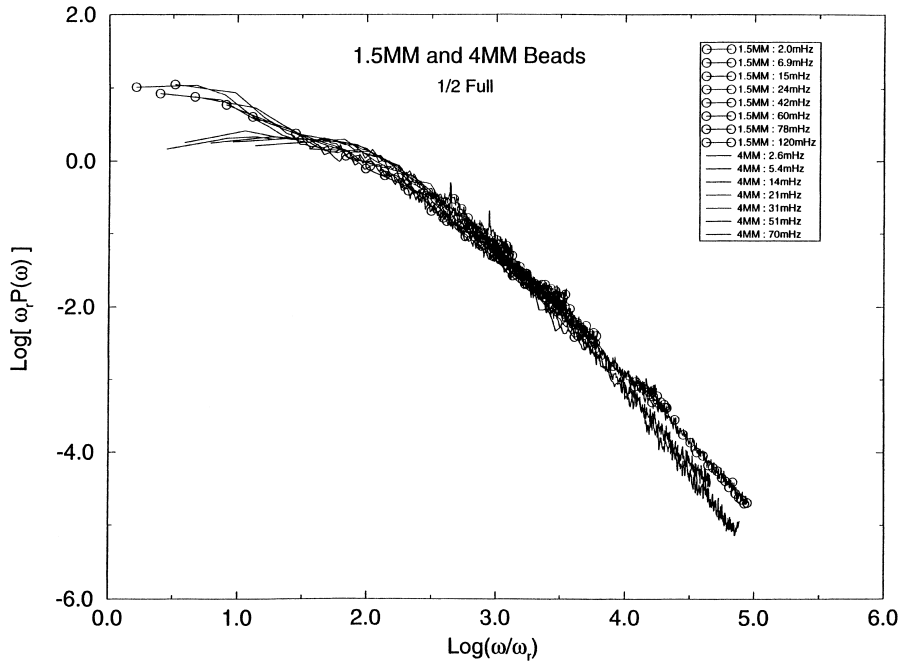

Fig. 5. Scaled power, $\dot{\theta}P(\omega/\dot{\theta})$, vs. scaled frequency, $\omega/\dot{\theta}$, for $d = 1.5$ and 4 mm, demonstrating rate independence. The scaled spectra for different grain sizes are similar over the parameter ranges considered here, except perhaps at low ω.

This figure also demonstrates that the exponent α for the low-ω portion of the spectrum lies in a range that may include 0. If $\alpha \equiv 0$, then these spectra would be simply explained by the fact that the power spectrum of a series of jumps in the stress varies as ω^{-2} at high frequency, and is flat below the frequency corresponding to the time between jumps. There is some indication, however, that $\alpha > 0$, a fact that would require a deeper understanding of the dynamics. Results discussed below for a 2D system may provide some insight into why $\alpha > 0$, and we will return to this point later.

Because the spectra are rate invariant, it is reasonable to compare the distribution of stresses observed in the experiment to the distributions predicted by theories such as lattice models developed for static configurations. Specifically, it is possible to think of the shearing as producing an ensemble of states consistent with the control parameters such as the mean density, particle size/type, etc. We then bin time-series stress data, $\sigma(t)$ without regard to temporal order to obtain distributions such as those given in Fig. 6. In these figures, the data points are connected by a line, and a fit to the q-model is given by the open circles. Except for the largest particles, the data are well described by an exponential at large stresses, and a leading power law. However, it is important to note that the data for the smaller particles are averages over many contacts. The number of these contacts varies as $N \propto d^2$, where d is the particle diameter. If each contact were uncorrelated from its neighbors and had the distribution ρ_q above, the force distribution for N such particles would be $\rho_N = (F_o(3N-1)!)(F/F_o)^{3N-1}\exp(-F/F_o)$. This distribution narrows as $N^{-1/2}$. But the data narrow more slowly than this, if at all. This lack of narrowing with decreasing d suggests the existence of correlations/anticorrelations between neighboring particles, so that the majority of the force reaching the transducer comes from a relatively small fraction of the particles.

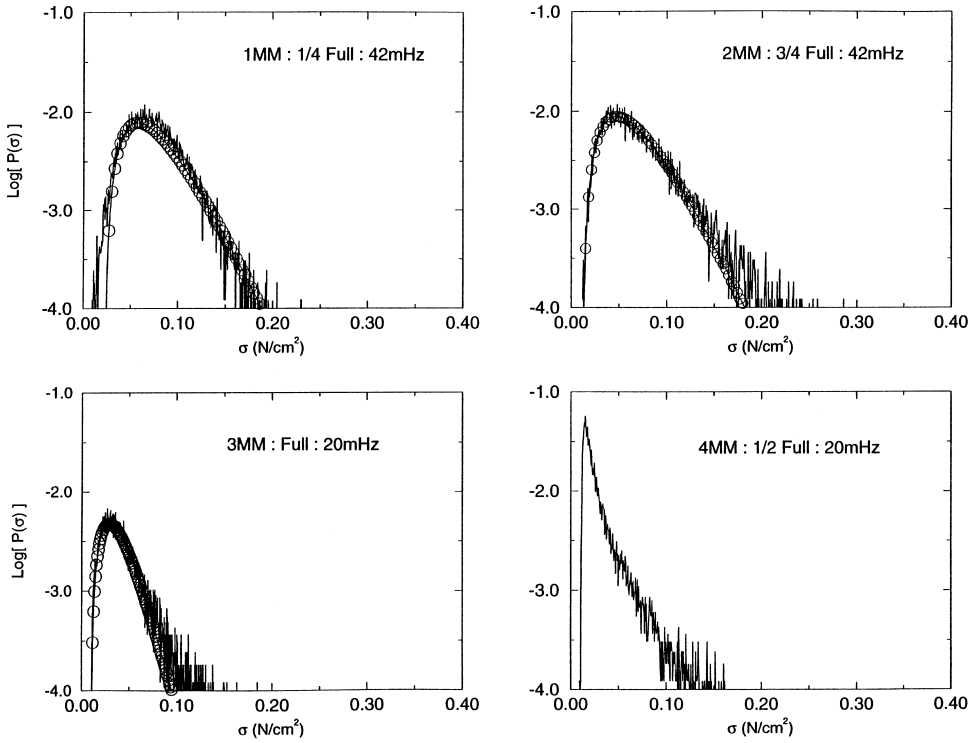

Fig. 6. Distributions for σ, normalized by the mean stress $\langle\sigma\rangle$, for different grain sizes but comparable rotation rates. A small positive quantity has been added to the ρ's in order to keep the logarithm finite. The circles indicate least squares fits to the form $\rho = A(\sigma - \sigma_{\text{offset}})^2 \exp(-\sigma/\sigma_0)$, as suggested by the analysis of Liu et al. and Coppersmith et al. The data for $d = 4$ and 5 mm did not fit well to the model because the relatively sharp rise for small σ.

2.2. A 2D granular material

It would be particularly valuable to know details of forces and displacements on individual grains in a shearing experiment. In 3D this is very difficult to achieve, and usually information is only available at boundaries [24]. However, it is possible to probe a 2D system much more extensively, Several quasi-static experiments have been carried out in 2D using the photoelastic effect [16]. Specifically, the experiments typically used disks, lying in a plane, and subject to stresses from the side. A photoelastic material is birefringent under stress/strain, so that if it is placed between crossed polarizers, light and dark regions appear. A much better polarizer uses circular polarization. Then the exiting intensity of a light ray that travels along the axial direction of a disk is $I \propto \sigma_2 - \sigma_1$, where the σ_i are the planar principal stresses in the disk along the path of the ray. It is a difficult task to infer detailed information about a large array of disks using photoelasticity. We address this difficulty by noting that localized contact forces on a grain lead to a series of bright and dark bands in the polariscope image of the disk. The number of bands is a function of the force at the contact. We use a technique that is effectively a measure of the number of such bands and hence the force on the contact. Specifically, we compute the square magnitude of the spatial gradient of the polariscope image intensity, $G^2 \equiv |\nabla I|^2$, and integrate this intensity on the scale of a particle (or larger in some cases). We can confirm by direct measurement that this quantity is a monotonic function of the applied force, as shown in Fig. 7. The response G^2 of a small number of disks is a linear function of a known applied force to a good approximation in the range of forces studied here. Indeed, the limitation on the linear regime is actually set by the spatial resolution of the camera and not by the technique itself.

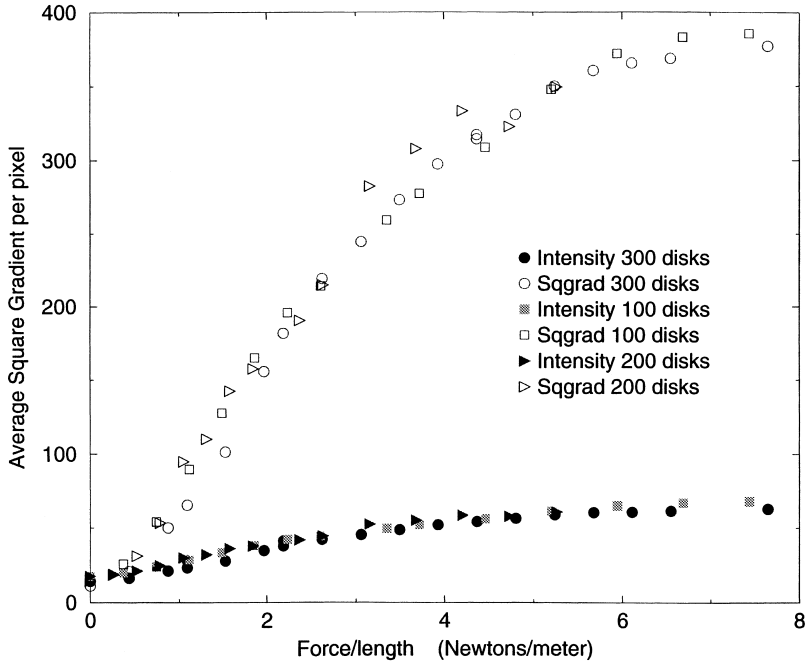

Fig. 7. Calibrations carried out on a few 100's of grains of the force vs. either G^2 (top data) or vs. the intensity (bottom data). The force was applied to the perimeter of the collection of grains. Typically, the applied force lies well within the linear region of G^2 vs. F/L.

We use photoelasticity and particle tracking to characterize the slow shearing in a 2D Couette system. The grains, i.e. disks, rest on a smooth slippery sheet, and are confined at the outer and inner radii by roughened surfaces, Fig. 2(b). Although, in principle, we can shear from either the inner or outer radii, we focus here only on shearing from the inner radius. The resulting dynamics of this system are quite complex, and we focus here on some of the key qualitative features, and an interesting transition that occurs as the packing fraction of disks, γ, is changed.

Several features are typical for almost all packing fractions. A characteristic shear band forms near the inner wheel, whose width, though dependent on γ, is usually about 6 disks in the radial direction. Virtually all the azimuthal motion of the disks occurs in this band, and the remaining outer disks remain nearly frozen. The mean (i.e. time averaged) azimuthal velocity, $V_\theta(r)$, is approximately exponential in the distance, r, from the inner wheel, as seen in Fig. 8. The disks within the shearband dilate, compacting disks in the outer region of the experiment. The velocity and spin distributions (i.e. particle rotation), Fig. 9, have a relatively complicated structure. Although in the mean, the dynamics of this system are relatively uniform, at any instant, the system is usually not at all homogeneous, and regions showing large stresses at one instant can be relatively stress free at other times. Fig. 1 shows an image of the experiment at a large packing fraction, $\gamma \simeq 0.80$, where the stresses are the most homogeneously distributed.

Of particular interest is the transition that occurs as γ is varied near $\gamma_c \simeq 0.77$. This critical γ corresponds to the density at which the system will have some stress at any time. For lower packing fraction, there will be no stresses in the system after initial transient relaxation in which the disks are pushed away from the inner shearing wheel. As γ increases above γ_c, the mean stresses within the system increase. Typical time series, Fig. 10, for the stress on a small subset of disks ($\sim$ 200 disks) show that near γ_c there are only intermittent "stress events". As γ increases above γ_c, the fluctuations are continuous in time and large. Interestingly, power spectra for these time series, Fig. 11, resemble those seen in the 3D shearing experiments of Miller et al. [22]. That is, these spectra, with the possible exception of one very near γ_c, show a high-frequency dependence $\propto f^{-2}$, and a low-frequency dependence that also appears to be a power law, but with an exponent, $0 < \alpha < 2$. Specifically, we do not see signs that the spectra

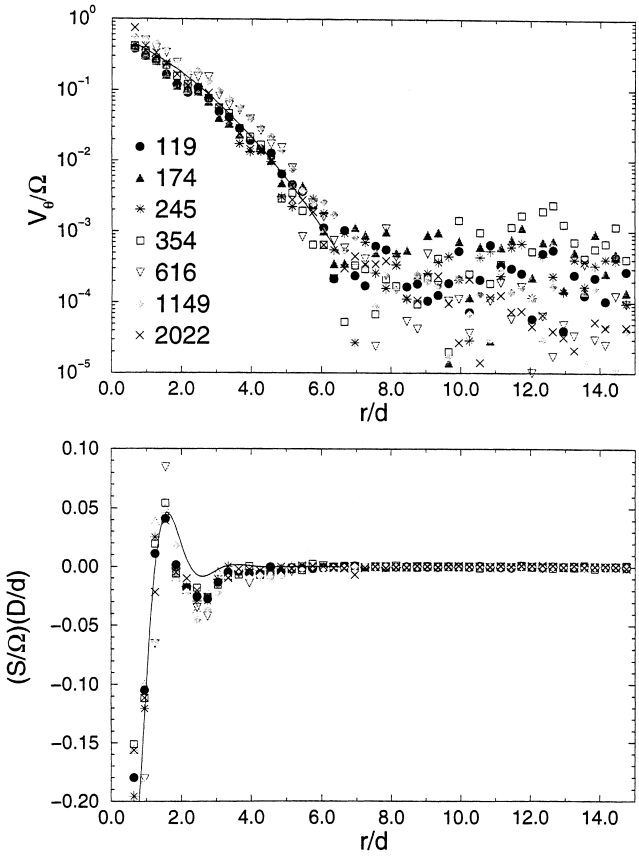

Fig. 8. Mean azimuthal velocity and mean spin for different rotation times. The symbols refers to different values of the rotation time τ in seconds. $\gamma = 0.788$. The solid lines correspond to the fits described in the text.

flatten at the lowest frequencies studied. A possible explanation may be that the grains in the outer regions undergo rearrangements on very slow time scales, a process that likely occurs in the 3D experiments as well.

The distributions of forces/stresses on the disks, Fig. 12, also show interesting changes as γ increases above γ_c. For moderate γ, the distributions shows exponential falloff, as in various lattice models. At large γ, there are clear signs of saturation, as many grains begin to take up the applied force. This approach to a more uniform distribution occurs because as the applied load increases, grains bearing the largest forces deform. Then neighboring grains can also absorb some of the force. For $\gamma \simeq \gamma_c$, the distributions are qualitatively different from the lattice model predictions.

We also show force distributions for $\sim 2 \times 10^2$ particles taken together, in order to compare with the data of Miller et al. Fig. 12(b) shows how these distributions change with γ. For moderate γ, these distributions fall off exponentially with force; for larger γ, they become narrower and more gaussian, and for near-critical γ's they vary rapidly with force, although the functional form is not clear. The data at moderate γ is consistent with the 3D force distributions of Miller et al. discussed above. These many-particle results cannot be directly compared to the q-model or similar models, since the distributions given by these models are for a single particle. However, for $N \sim 10^2$ particles, the distributions should show narrowing as $N^{-1/2}$ if the forces were uncorrelated, as discussed above. However, the experimental distributions in 2D do not show this narrowing, except at large γ. We believe that the underlying reason for the lack of narrowing is the existence of correlations. Thus, very near γ_c stress chains are

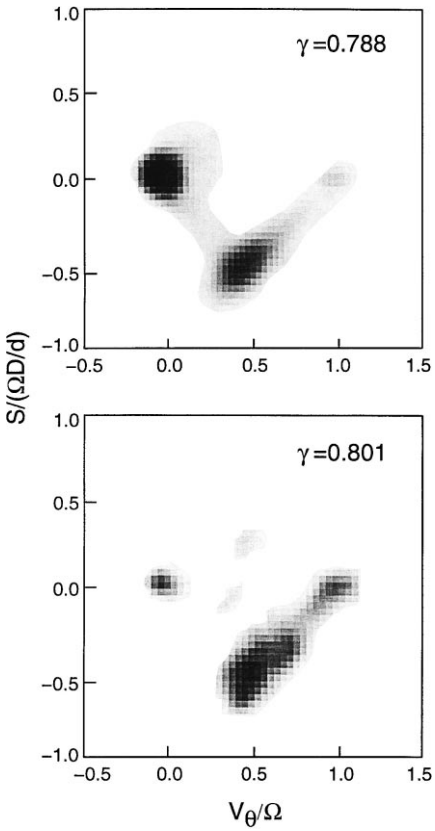

Fig. 9. Greyscale representation of the 2D probability density for V_θ/Ω and $S/(\Omega D/d)$ for $0 < r/d < 1$. Data are shown for two indicated values of γ.

long and radially oriented. For increasingly larger γ, the chains begin to branch, run in all directions, and become more tangled, so that the characteristic length of a straight line portion becomes much shorter. We are currently working to determine the distribution of chain segment lengths quantitatively. However, it is visually clear that the mean segment length, $\bar{L}$, becomes large as $\gamma \to \gamma_c$. The reason for this is that near γ_c, the system is very compressible. Hence, a stress chain is susceptible to buckling within the interior. Rather than splitting, latent chains will simply slip or buckle. Chains running from boundary to boundary with the grains aligned in a nearly straight line are most likely to be stable. As γ increases, the system becomes more rigid and chains are less likely to buckle.

3. Friction-shaking

Another aspect of granular flow is the stability of material when it is shaken. For instance, if a layer of granular material is shaken strongly enough horizontally, then we expect on the basis of simple Coulomb friction that the material will undergo frictional failure on a horizontal plane somewhere in the material. This picture of granular failure is the basis for much practical design [14,15].

One way to investigate this kind of behavior is through the application of shaking. Here, we consider experiments in which sinusoidal shaking is applied independently in the vertical and horizontal directions:

$$s_i = A \sin \omega_i t, \tag{1}$$

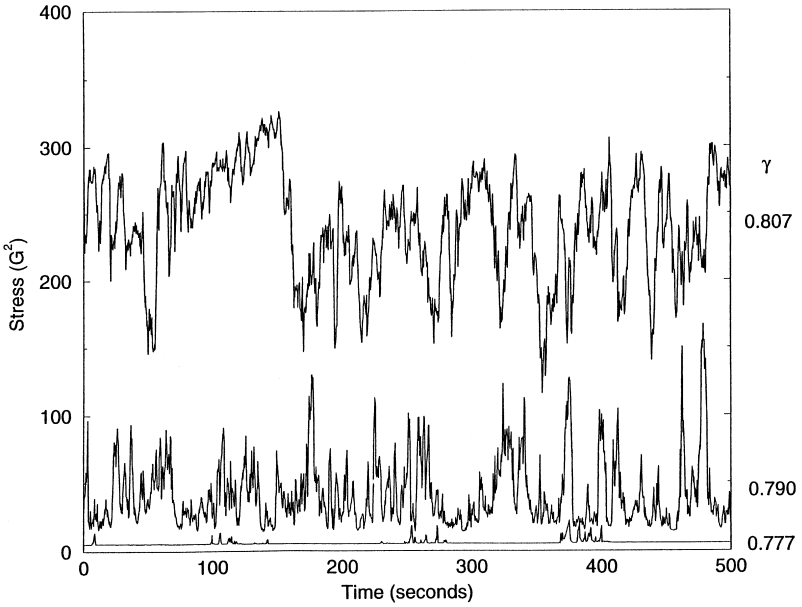

Fig. 10. Time series, G^2 vs. t, for ~ 200 particles. Different sets correspond to different packing fractions ranging from $\gamma < \gamma_c$ (bottom set) to densely packed conditions (top set).

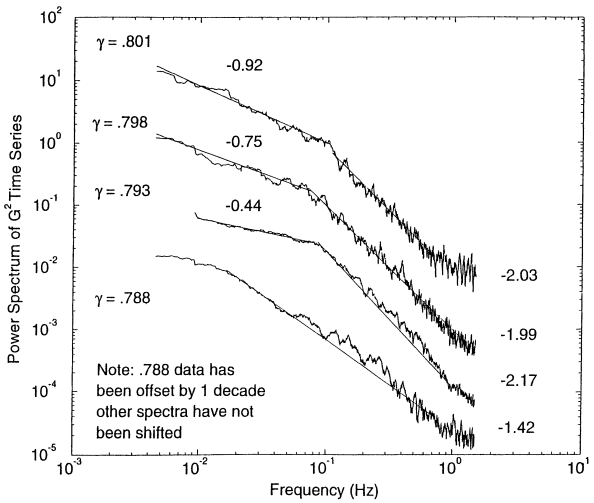

Fig. 11. Power spectra from times series for G^2 for the indicated γ's. Here, roughly 200 grains were imaged. The numbers indicated the exponents of the low and high frequency regimes, as determined by least squares fits.

where $i = \mathrm{h}, \mathrm{v}$ for horizontal or vertical shaking. The relevant control parameters include the two dimensionless accelerations, $\Gamma_i \equiv A_i \omega_i^2$.

We have carried out experiments to probe the initial flow states as Γ_h is increased quasi-statically from zero. The material remains stationary up to Γ^* (Fig. 13) as one would expect on the basis of Coulomb friction. Above this Γ_h, the material sloshes back and forth in the direction of shaking. In addition, there is a transverse flow, i.e. in the horizontal plane perpendicular to the shaking direction. This transverse flow is due to shear at the boundary, as we show elsewhere [31]. However, if Γ_h is then decreased, the transition back to the no-flow state is hysteretic (Fig.

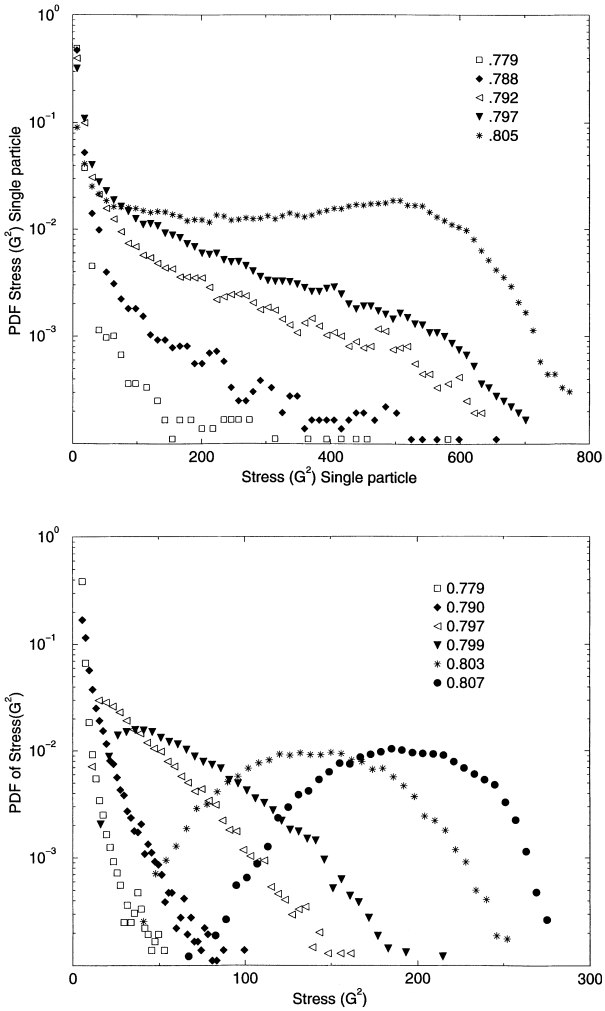

Fig. 12. (Top) Distributions of G^2, i.e. forces, on single particles near the shearing wheel for the indicated γ's. (Bottom) Distributions of G^2 for ~ 200 particles at a time.

13), i.e. it occurs for $\Gamma_h = \Gamma_c < \Gamma^*$. This hysteresis is not so easily explained in the context of Coulomb friction. Moreover, by passing a gentle fluidizing stream of gas vertically through the layer, the hysteresis is removed, as shown in Fig. 14. At the point where the data for Γ^* and Γ_c merge, the dilation of the sample is only about 2%.

In a second set of experiments, we have provided shaking in both the vertical and horizontal directions independently. In this case, the possible set of dynamics can be quite complex, and there are a number of different dimensionless control parameters besides just the Γ_i. One of the most important of these is the phase difference, ϕ, between the two components of shaking. Here, we will focus just on the case $\phi = 0$; a brief discussion of the case $\phi \neq 0$ is given elsewhere [32].

Key issues explored in these experiments are the concept of Coulomb friction and the idea of fabric. In its most basic form, Coulomb friction as applied to these experiments, is captured by a frictional block on a plane inclined at angle θ, as in the inset of Fig. 15. We imagine that the block corresponds to a chunk of material and we ask whether static friction can keep it in place under applied shearing, normal and gravitational forces. The base on which the block rests is accelerated in the horizontal and vertical directions, as $\vec{a} = \hat{x} g\Gamma_h + \hat{z} g\Gamma_v$. For instance, if

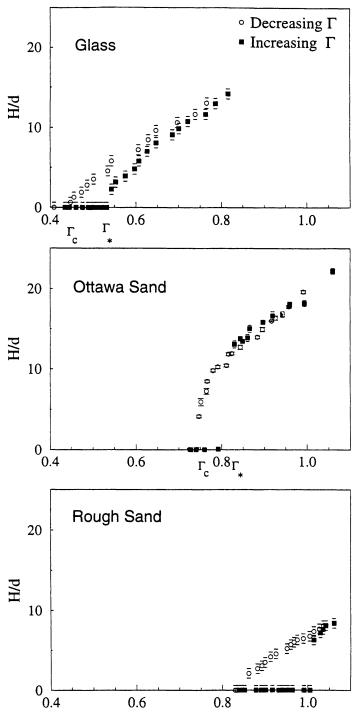

Fig. 13. Thickness of the liquefied layer versus acceleration amplitude Γ for glass beads, $d = 0.6$ mm and rough sand $d_{ave} = 0.6$ mm. Γ^* and Γ_c are the bifurcation points when Γ is increased and decreased quasi-statically.

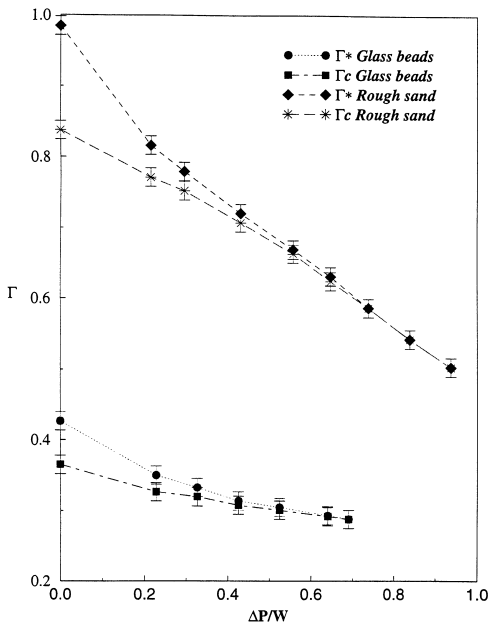

Fig. 14. Bifurcation points Γ^* and Γ_c versus dimensionless lifting pressure for rough sand and for glass beads.

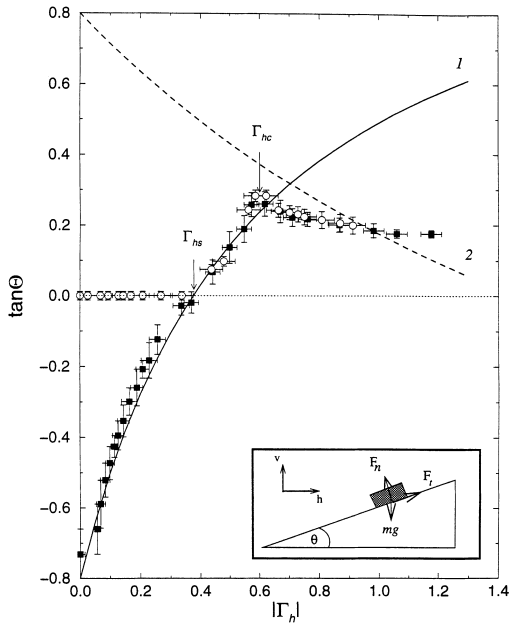

Fig. 15. Inset: sketch of inclined surface that defined the model. Open circles: heap angle, θ of a thick (58 mm) Ottawa sand bed as a function of $\Gamma_{\rm h}$, for $\Gamma_{\rm v} = 0.68$ for in-phase ($\Phi = 0$) horizontal and vertical forcing ($f_{\rm h} = f_{\rm v} = f = 4.99\,{\rm Hz}, A_{\rm v} = 6.77\,{\rm mm}, A_{\rm h}$ varying), starting from a flat surface. Solid squares: same control parameters, but starting from a heap against the left wall at the angle of repose. Lines pertain to the model curve $1 : \Gamma_{\rm h,v} < 0$, and curve $2 : \Gamma_{\rm h,v} > 0$, with $\mu = 0.80$ and $\Gamma_{\rm vc} = 1.15$. Error bars in this and other figures were obtained from ~ 3 repetitions of the experiment.

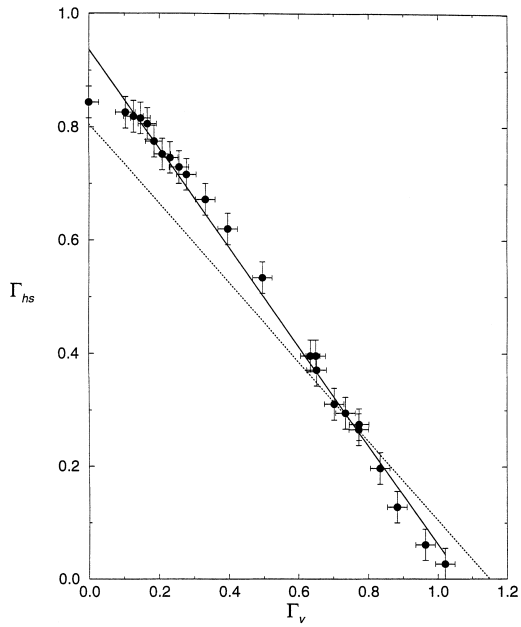

Fig. 16. Data for $\Gamma_{\rm hs}$ vs. $\Gamma_{\rm v}$. According to the model, these data should have slope $-\mu$ and intercept $\Gamma_{\rm vc} = 1$. Solid curve: least squares fit of the experimental data ($\mu = 0.87$; $\Gamma_{\rm vc} = 1.07$); dotted curve: model with $\mu = 0.80$ and $\Gamma_{\rm vc} = 1.15$.

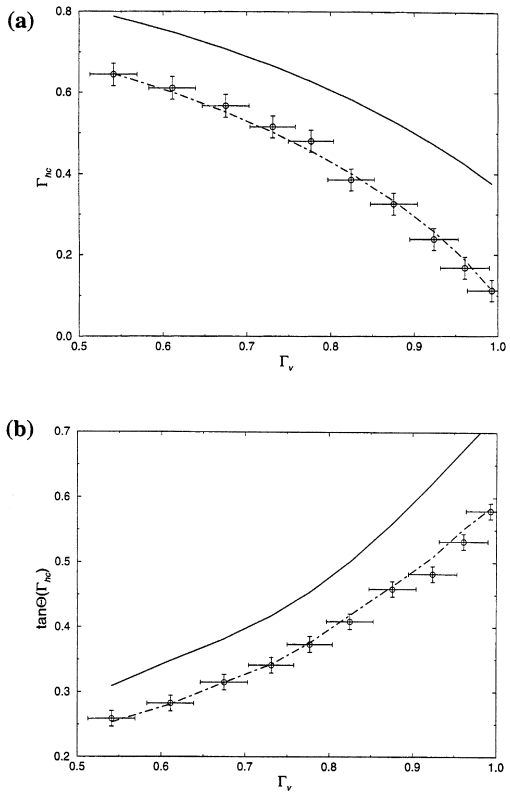

Fig. 17. Points: data for (a) Γ_{hc}, and (b) $\tan\theta$ at Γ_{hc} vs. Γ_v. Solid curve show predictions of the Coulomb friction model for $\mu = 0.80$ and $\Gamma_{vc} = 1.15$. Dot-dashed curve in (a) is for $\mu = 0.77$ and $\Gamma_{vs} = 1.03$ and in (b) is for $\mu = 0.65$ and $\Gamma_{vc} = 1.35$.

$\Gamma_v < 0$, the normal forces on the block, F_n, and hence the maximum static friction force, F_f are reduced, so that the block can slip more easily under a horizontal acceleration. If $\Gamma_v > 0$, the block is stabilized against slipping, but for large enough horizontal accelerations, slipping must still occur. The two curves in Fig. 15 show $\tan\theta$ as function of $|\Gamma_h|$ at which slipping occurs, where curve 1 applies for downward acceleration, and curve 2 applies for upward acceleration. This simple picture does not fully account for the fact that the grains are interlocking. The actual forces on a layer of material are sensitive to the details of this interlocking, and therefore to the history of the sample. This aspect of granular materials is known as fabric.

We now apply these ideas to a sample of material in which the vertical and horizontal accelerations are not constant but are oscillating sinusoidally in time with peak values Γ_i. If the frequencies of oscillation are not too great, the grains will accelerate and move in such a way that the peak accelerations determine the dynamics of the system.

If a flat horizontal layer of material is oscillated with $0 < \Gamma_v < 1$, and Γ_h is gradually increased from 0, we find that the layer undergoes a novel instability at $\Gamma_h = \Gamma_{hs}$ to a new static state in which the material forms a static inline of slope $\tan\theta$. Typical data are given by the open symbols in Fig. 15. If Γ_h is further increased at constant amplitude Γ_v, a second transition occurs at Γ_{hc} to a state in which the grains slosh back and forth on the surface. We qualitatively understand these observations in terms of Coulomb friction fairly simply. The transition to an inclined static heap at Γ_{hs} occurs because at the most negative downward acceleration, frictional failure will first occur at $\tan\theta = 0$ when curve 1 crosses the Γ_h axis. However, an inclined heap can still be stable against slipping up to the point where curves 1 and 2 cross. Hence, with increasing Γ_h, the heap will evolve up to the slope of curve 1

in the range $\Gamma_{hs} < \Gamma_h < \Gamma_{hc}$. Above the crossing point of curves 1 and 2, slipping must (and does) occur in both directions, and sloshing results. We test this picture additionally by preparing a heap at the angle of repose of the system, and we then sweep Γ_h upward from 0. In this case, we obtain the solid symbols of Fig. 15. The analytic forms of curves 1 and 2 are given by

$$\tan\theta = (\Gamma_h - \Gamma_{hs})/(1 - \Gamma_v + \mu\Gamma_h), \tag{2}$$

(curve 1), and

$$\tan\theta = -(\Gamma_h - \mu(1 + \Gamma_v))/(1 + \Gamma_v + \mu\Gamma_h), \tag{3}$$

(curve 2), where we use $\Gamma_{hs} = \mu(\Gamma_{vc} - \Gamma_v)$. There is only one unknown parameter in these equations, namely μ, the static friction coefficient, since $\Gamma_{vc} \equiv 1$.

We can test this picture additionally, Figs. 16 and 17, by measuring Γ_{hs}, Γ_{hc}, and $\tan\theta$ at Γ_{hc} as functions of Γ_v. For instance, data for Γ_{hs} versus Γ_v, Fig. 16, show nearly the expected straight line predicted by Coulomb friction, but the $\Gamma_{hs} = 0$ intercept does not appear to occur exactly at $\Gamma_v = 1$, presumably because there is grain interlocking that is not totally accounted for by static friction. We can make a small modification to the model in which we choose $\Gamma_{hs} = \mu(\Gamma_{vc} - \Gamma_v)$, i.e. we choose Γ_{vc} independently with $\Gamma_{vc} > 1$ to better reflect this effect. It is this choice of Γ_{hs} that we use to fit the data in Fig. 15. Further, we can compare the model to data for Γ_{hc} and for the slope of the static heap at Γ_{hc}. Fig. 17 shows such a comparison. Although it is possible to fit one of these data sets to the model by adjusting μ and Γ_{vc}, it is not possible to get everything quantitatively right with the same set of parameters.

4. Conclusions

Granular materials present a number of predictability challenges. One of the traditional elements used for understanding granular materials is Coulomb friction, which contains a significant element of unpredictability. To move beyond Coulomb friction requires more information on the history of a sample or of its internal variables. In the final example considered here, friction was able to predict the transitions to heaping and flow qualitatively but not quantitatively.

Another modeling issue, one that has been traditionally neglected, is fluctuations. In laboratory systems that have dimensions 10^1 to 10^2 grain diameters, these fluctuations are enormous – i.e. often an order of magnitude greater than the mean. It is therefore very important to understand how these fluctuations scale with size and history. In the experiments presented at the beginning of this work, we considered a 2D system in which we determined the stress and velocity fluctuations associated with slow shear. A key finding here is the dependence of these fluctuations on the density of this system. In particular, there is a critical packing fraction, γ_c, below which the stresses fall to zero. Just above γ_c, fluctuations are temporally intermittent, and the resulting stress chains tend to be long. As γ is increased further, the system becomes more homogeneous because strong contacts now deform enough to allow other contacts to take up the load. As a result, the stress network becomes more tangled and has more branches, with effectively a shorter characteristic length in the system. The intermediate range of γ is typically what occurs in a dense packing of hard grains for moderate applied loads. Here, there are contacts throughout the system, but the applied loads are not so great that the force is distributed more uniformly among the contacts. The observed force distributions are roughly as predicted by several models. However, it is clear that there are spatial correlations in the experiment that are important.

Acknowledgements

CV and RPB appreciate the hospitality of the École supérieure de Physique et Chimie Industrielle – P.M.M.H. where some of this work was carried out. The work of DH and RPB was supported by the NSF grants DMR98-02602 and DMS-9803305, and by NASA under Grant NAG3-1917.

References

[1] H.J. Herrmann, S. Luding, J.P. Hori (Eds.), Dry Granular Media, Nato ASI series, Kluwer Academic Publishers, Amsterdam, 1998.
[2] R.P. Behringer, J.T. Jenkins (Eds.), Powders and Grains 97, Balkema, Rotterdam, 1997.
[3] H.M. Jaeger, S.R. Nagel, R.P. Behringer, Physics Today 49 (1996) 32.
[4] H.M. Jaeger, S.R. Nagel, R.P. Behringer, Rev. Mod. Phys., 68 (1996) 1259 and references therein.
[5] D. Bideau, J. Dodds (Eds.), Physics of Granular Media, Les Houches Series, Nova, 1991.
[6] A. Mehta (Ed.), Granular Matter: an Interdisciplinary Approach, Springer, NY, 1994.
[7] R.P. Behringer, Nonlinear Science Today 3 (1993) 1.
[8] I. Goldhirsch, G. Zanetti, Phys. Rev. Lett. 70 (1993) 1619.
[9] S. McNamara, W.R. Young, Phys. Rev. E 53 (1996) 5089.
[10] E.L. Grossman, Tong Zhou, E. Ben-Naim, Phys. Rev. E 55 (1997) 4200.
[11] P.K. Haff, J. Fluid Mech. 134 (1983) 401.
[12] C.H. Liu, S.R. Nagel, Phys. Rev. Lett. 68 (1992) 2301.
[13] C.T. Veje et al., Dry Granular Media, H.J. Herrmann, S. Luding, J.P. Hovi (Eds.), Nato ASI series, Kluwer Academic Publishers, Amsterdam, 1998; Phys. Rev. E 59 (1999) 739.
[14] R. Jackson, in: Re. E. Meyer (Ed.), Theory of Dispersed Multiphase Flow, Academic Press, NY, 1983, p. 291.
[15] R.M. Nedderman, Statics and Kinematics of Granular Materials, Cambridge, 1992.
[16] P. Dantu, Géotechnique 18 (1968) 50.
[17] A. Dreshcer, G. De Josselin De Jong, J. Mech. Phys. Solids 20 (1972) 337.
[18] T. Travers et al., J. Phys. A. 19 (1986) L1033. R.B. Heywood, Designing by Photoelasticity, Chapman and Hall, London, 1952.
[19] G.W. Baxter, R.P. Behringer, Eur. J. Mech. B 10 (1991) 181.
[20] G.W. Baxter, R. Leone, R.P. Behringer, Europhys. Lett. 21 (1993) 569.
[21] D.G. Schaeffer, J. Diff. Eq. 66 (1987) 19.
[22] B.J. Miller, C.O'Hern, R.P. Behringer, Phys. Rev. Lett. 77 (1996) 3110.
[23] A. Ngadi, J. Rajchenbach, Phys. Rev. Lett. 80 (1998) 273.
[24] D.K. Muth, H.M. Jaeger, S.R. Nagel, Phys. Rev. E 57 (1998) 3164.
[25] C.-h. Liu, S.R. Nagel, D.A. Schecter, S.N. Coppersmith, S. Majumdar, O. Narayan, T.A. Witten, Science 269 (1995) 513.
[26] C.-h. Liu, S.R. Nagel, D.A. Schecter, S.N. Coppersmith, S. Majumdar, O. Narayan, T.A. Witten, Phys. Rev. E 53 (1996) 4673.
[27] P. Claudin, J.-P. Bouchaud, Phys. Rev. Lett. 78 (1997) 231.
[28] M. Nicodemi, Phys. Rev. Lett. 80 (1998) 1340.
[29] J.E.S. Socolar, Phys. Rev. E 57 (1998) 3204.
[30] F. Radjai, M. Jean, J.-J. Moreau, S. Roux, Phys. Rev. Lett. 77 (1996) 274.
[31] S.G.K. Tennakoon, L. Kondic, R.P. Behringer, Europhys. Lett. 45 (1999) 470.
[32] S.G.K. Tennakoon, R.P. Behringer, Phys. Rev. Lett. 81 (1998) 794.